# A Novel Topology of Single Phase to Three Phase Power Converter with Active Input Current Shaping

N. Tejaram[1], Dr. CH. Chengaiah[2]
[1]*Student of Master of Technology, Department of Electrical & Electronics Engineering, Sri Venkateswara University College of Engineering, S V University, Tirupati, India*
[2]*Professor, Department of Electrical & Electronics Engineering, Sri Venkateswara University College of Engineering, S V University, Tirupati, India*

***Abstract*** **- This paper presents a converter topology for driving a three-phase motor load from a single-phase supply. It consists of a rectifier and an inverter circuit. The front-end rectifier is to provide a DC link voltage through a split capacitor. The two-leg inverter converts this DC link voltage into 3 phase supply. This converter can run a three-phase Induction motor which is much more efficient compared to a single-phase motor. In this paper, two closed-loop controllers are employed to achieve balanced output voltage. Among those two closed-loop controllers, one is for maintaining the DC link voltage constant and, the other is for inverter output. Therefore, the single-phase to three-phase converter brings the controllable output voltage as in a six-switch standard three-phase inverter. The front-end rectifier has the capability of active input current shaping. The designed converter model is simulated by using MATLAB Simulink software. The Performance of the designed converter employing various controllers like PI and Fuzzy Logic is assessed.**

***Index Terms*** **- Front-end rectifier, Split-Capacitor, DC-Link voltage, Two-leg Inverter, Three-phase motor.**

## 1.INTRODUCTION

Access to energy is a cornerstone for development and essential for a better quality of life. When this access doesn't exist or is very poor, it has negative impacts on everything from education, health, employment, and irrigation - touching all aspects of life and livelihood. The single-phase power has been alternative for rural areas or remote areas. Most of the remote areas have access to single phase power. On the other hand, three-phase electric motors have several advantages compared to single-phase electric motors. The performance of three-phase motor drive systems is superior when compared with single-phase motor drives. The three-phase motors are more efficient, low cost, and less output torque ripples [8]. Therefore, a bridge capable of connecting single-phase power to three-phase appliances is required. In the past, single-phase to three-phase conversion systems were made possible by the connection of passive elements (capacitors and reactors) with autotransformer converters [4]. Such kind of system presents well-known disadvantages and limitations. The power electronics with silicon-controlled rectifiers began emerging in the market from the early 1960s. A breakthrough in the field of power electronics came up with the invention of MOSFET and IGBT. There also been the great innovations in circuit topology in the field of power conversion systems was also identified [2].

## 2. CONVENTIONAL SINGLE PHASE TO THREE PHASE CONVERTERS

The conventional topology includes the converter, which can either be full bridge type, or half bridge type, with a DC link capacitor in cascade with a three-phase inverter [9]. In the conventional converters the AC-to-DC conversion is independent from the DC-to-AC conversion. The converter connected to the supply is called the lineside converter and the one connected to the load is the load-side converter. Therefore, in the conventional topologies the control of the line and the load side converters are independent.

### A. Conventional full bridge topology

The conventional topology for single-phase to three-phase power converter shown in figure 1 employs a diode bridge rectifier and a regular six switch PWM inverter. The full bridge topology has four switches for the AC to DC conversion.

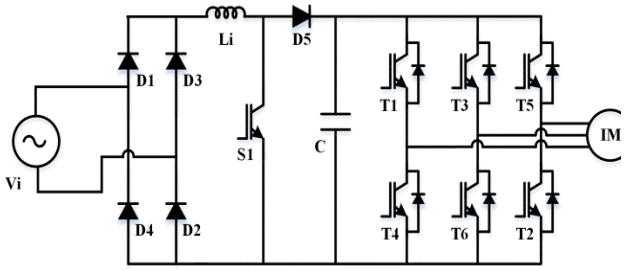


Fig. 1 Conventional single-phase to three-phase converter for ac motor drives.

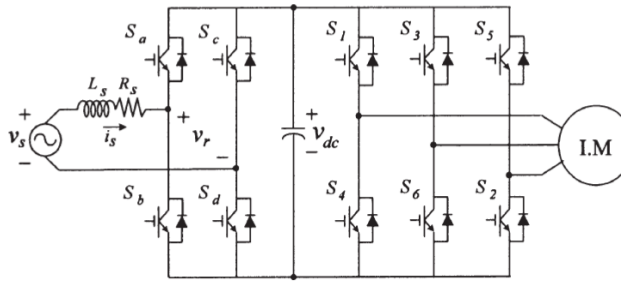


Fig. 2 Conventional single-phase to three-phase converters for AC motor drives with input current shaping

**B. Conventional half-bridge topology**

The half bridge topology shown in figure 3 is like a full bridge topology except that a capacitor leg with neutral accessible replaces one of the converter legs of the line side converter, but the load side converter remains the same.

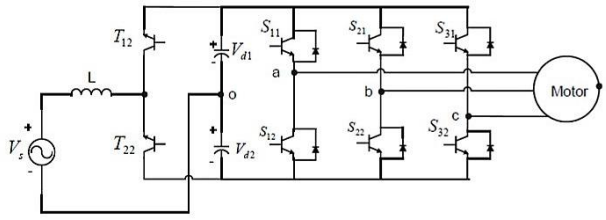


Fig. 3 Conventional Half bridge rectifier circuit single-phase to three-phase converter.

The irregular power distribution among the switches of the converter is shown in the figure 4. It means that 63% of the total losses measured in the single-phase to three-phase converter is concentrated in the rectifier circuit, while the rest 37% is observed in inverter circuit. With those numbers, it is possible to measure the stress by switch, which means that each rectifier switch is responsible for 15.7% of the total converter losses, while each inverter switch is responsible for only 6.1% [2]. The stress by each switch gives an important parameter regarding the possibilities of failures in the power converter. Therefore, the reduction in components leads to more efficiency of the converter.

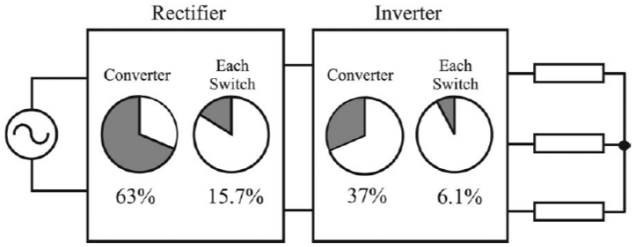


Fig. 4 Converter power losses distribution in both rectifier and inverter units.

## 3. PROPOSED SINGLE PHASE TO THREE PHASE CONVERTER

The proposed single-phase to three-phase converter shown in figure 5 which employs only six transistor or IGBT type switches. The proposed configuration incorporates a front-end half bridge active rectifier structure which provides the DC-link with active input current shaping feature. Further, the front-end rectifier allows bi-directional power flow between the DC-link and the AC mains. A four-switch inverter configuration with split capacitors in the DC-link provides a balanced three phase output to the AC motor load.

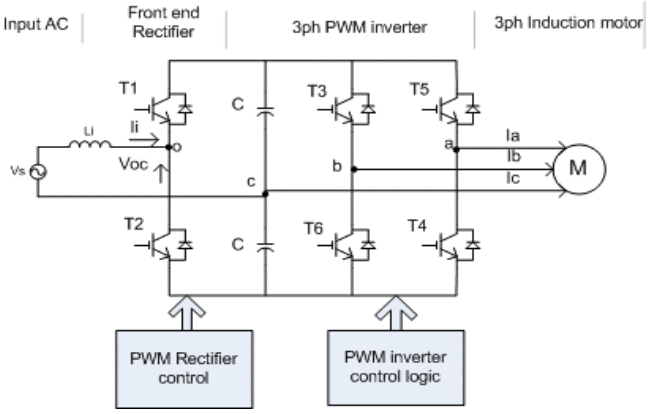


Fig. 5 Proposed single-phase to three-phase converter

**A. Converter design**

The minimum inductance L that limits the ripple current $I_s$

$L_{min} = \frac{V_{in}*(V_o - V_{in})}{\Delta i_l * f_s * V_o}$ $L_{min} = 5$ mH

Where $f_s$ is the switching frequency and $V_{in}$ is the rms voltage.

The capacitor size is determined by the percentage of desirable ripple in each half of the DC-link voltage.

$C=\frac{V_{dc}}{f_s R_L V_r}$

$C$ =2.331 mF

Where C is the capacitance across half the DC bus and $R_L$ is the equivalent load resistance for rated power transfer. $V_{dc}$ is the DC bus voltage and $V_r$ is the percentage of ripple voltage.

**B. Front-end rectifier**

The single-phase AC input which is of fixed frequency is rectified by the front-end rectifier switches $T_1$ and $T_2$. The split capacitor bank in the DC-link is charged through the diodes present in $T_1$ and $T_6$. The switches $T_1$ and $T_2$ are operated on a PWM pattern synchronized to the AC mains to shape the input current to be sinusoidal. The filter inductor L, aids in filtering higher order current harmonics. The fundamental component of the voltage at points 'O' and C' is $V_{oc,1}$ which is essentially the reflected voltage due to the PWM operation of $T_1$ and $T_2$. Figure 6 shows the phasor diagram of the input voltage $V_{in}\angle 0$ and $V_{oc,1}\angle\theta$.

Where $\theta$ is the phase shift angle between the voltages $V_{in}$, and $V_{oc,1}$.

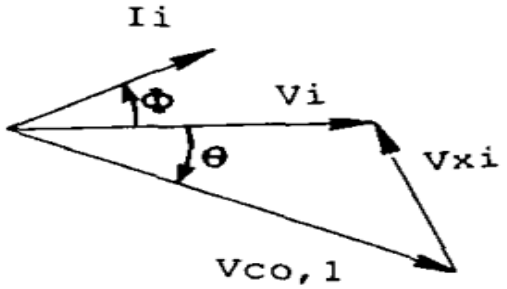


Fig. 6 Phasor diagram

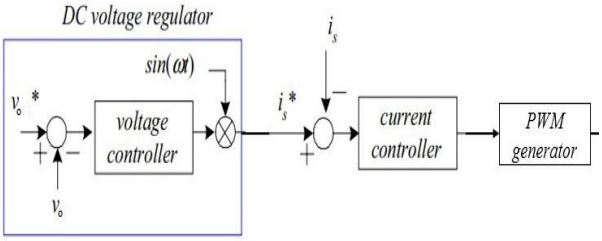


Fig. 7 Control strategy of Front-end rectifier

The input current $I_i$, is given by

$$I_i\angle\phi = \frac{V_{in}\angle 0 - V_{oc,1}\angle\theta}{jX_i} \quad (1)$$

The real power flowing from AC mains to the DC-link can be expressed as

$$Pi=\frac{V_{in}.V_{oc,1}sin\theta}{X_i} \quad (2)$$

The power factor angle is given by

$$\phi=\tan^{-1}\left(\frac{V_{in}-V_{oc,1}\cos\theta}{V_{oc,1}\sin\theta}\right) \quad (3)$$

The input power factor pf is given by

$$\cos\phi = \frac{V_{oc,1}*\sin\theta}{\sqrt{V_{in}{}^2+V_{oc,1}{}^2-2.V_{in}.V_{oc,1}.\cos\theta}} \quad (4)$$

A constant value of k implies that the DC-link voltage is regulated to maintain a constant value $V_o$, as given by

$$k = \frac{\sqrt{2}V_{oc,1}}{\sqrt{2}V_{in}} = \frac{V_o}{2\sqrt{2}.V_{in}} \quad (5)$$

To obtain close to unity input power factor and a regulated DC-link voltage $V_o$, it is proposed that we maintain k = 1 with the help of a voltage control loop. Maintaining k = 1 also implies that the DC-link voltage

$$V_o = 2\sqrt{2}V_{in} \quad (6)$$

**Control strategy of front-end rectifier**

The DC bus voltage controller shown in figure 7 is used to control the DC-link voltage and to obtain the amplitude of the line current command. Because the system input power factor is controlled to be unity, the output signal obtained from the proportional-integral based voltage controller is multiplied by a sinusoidal wave in phase with mains voltage. The line current command is used in the inner current control loop to achieve line current tracking [5].

The Front-end rectifier can be operated in two modes shown in figure 8.

1. Charging mode
2. Discharging mode

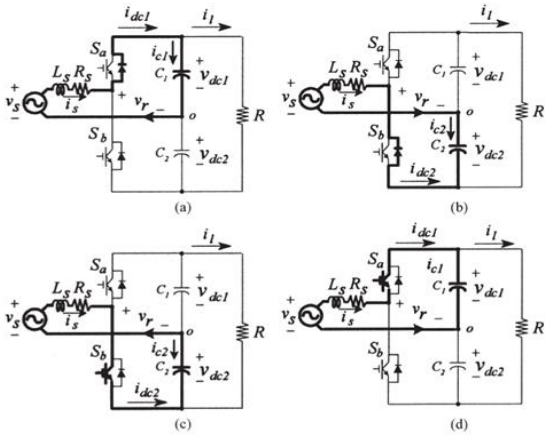

Fig. 8 Operating modes of the circuit. (a) and (b) Charging. (c) and (d) Discharging.

The Positive line current flows through boost inductor L, body diode of $T_1$, diode $D_1$ and capacitor $C_1$ such that, capacitor $C_1$ is charged by the line current. Because the half DC-link voltage is greater than the amplitude of mains voltage, the line current is decreasing linearly. During $i_s$>0, the

switch $T_2$ is turned ON the capacitor $C_2$ is discharged. When $i_s$>0, for the upper part of the rectifier, the current and voltage are given by

$$i_{c1} = i_{dc1} - i_l \quad (7)$$

$$i_{dc1} = S_a * i_s \quad (8)$$

$$V_{dc1} = \frac{1}{C}\int i_{c1}\mathrm{d}t = \frac{1}{C}\int (i_{dc1} - i_1)\mathrm{d}t \quad (9)$$

Where $S_a$ is a switching state, i.e., 1 or 0. For discharging part, the similar equations are obtained as follows:

$$i_{c2} = -i_{dc2} - i_l \quad (10)$$

$$i_{dc2} = S_b * i_s = (1 - S_a) * i_s \quad (11)$$

$$V_{dc2} = \frac{1}{C}\int i_{c2}\, dt = \frac{1}{C}\int (-i_{dc2} - i_l) dt \quad (12)$$

For $i_s$ < 0, the same equations can be applied to the relation of current and voltage.

By combining all the equations (7)-(12)

$$V_r = S_a * V_{dc1} - S_b * V_{dc2} \quad (13)$$

$$V_o = V_{dc1} + V_{dc2} \quad (14)$$

C. FOUR SWITCH THREE PHASE INVERTER

The output side of the proposed single-phase to three-phase converter consists of a four switch ($T_3$ to $T_6$) inverter. The centre point of the capacitors forms the third phase 'c'.

By controlling the switches $T_5$ and $T_4$ in a PWM fashion the output voltage $V_{ca}$ can be defined. Further, switches $T_3$ and $T_6$ determine the $V_{bc}$ voltage. To generate balanced three-phase output voltages, the voltage $V_{bc}$ is phase shifted by -60° from $V_{ca}$. Thus, the control of switches $T_3$ to $T_6$ to have 60° phase shift between $V_{ca}$ and $V_{bc}$, voltages ensure the third voltage $V_{ab}$ to have the same magnitude (fundamental) and proper phase in accordance with the three-phase laws It is noted that voltage $V_{ab}$ is a two level PWM swinging between $V_o$ and $-V_o$. On the other hand, the voltages $V_{ca}$ and $V_{ca}$ are two level type swinging between $+V_{o/2}$ and $-V_{o/2}$. Further, the fundamental content is the same in the three-phase output voltages.

D. Field oriented control of four switch three phase inverter topology

In general, torque control of a three-phase induction machine is not straight forward as that of a dc machine because of the interactions between the stator and rotor fields whose orientation are not held spatially at $90^0$ but vary with operating condition. The field of the rotor winding in an induction machine may be likened to that of a field winding of a dc machine, except that it being induced is not independently controllable. With sinusoidal excitation, the rotor field rotates at synchronous speed.

For very low-speed operations and for position type control, the use of flux sensing that relies on integration which tends to drift may not be acceptable. A commonly used alternative is indirect field orientation, which does not rely on the measurement of air gap flux, but uses the condition in equations (15), (16) and (17) to satisfy the condition for proper orientation. Torque can be controlled by regulating $\boldsymbol{i}^{e}_{qs}$ and slip speed. Rotor flux can be controlled by regulating $\boldsymbol{i}^{e}_{ds}$

The magnitude torque is

$$T_{em} = \frac{3}{2}\frac{P}{2}\frac{L_m}{L'_r}\lambda'^{e}_{dr} i'^{e}_{qr} \quad (15)$$

we obtain the following relationship between slip speed and the ratio of the stator $q_d$ current components for the d-axis of the synchronously rotating frame to be aligned with the rotor field.

$$\omega_e - \omega_r = -\frac{r'_r}{L'_r}\frac{i^e_{qs}}{i^e_{ds}} \quad (16)$$

$$i^s_{ds} = \frac{1}{\sqrt{3}} i_{as}(i_{bs} + i_{cs}) \quad (17)$$

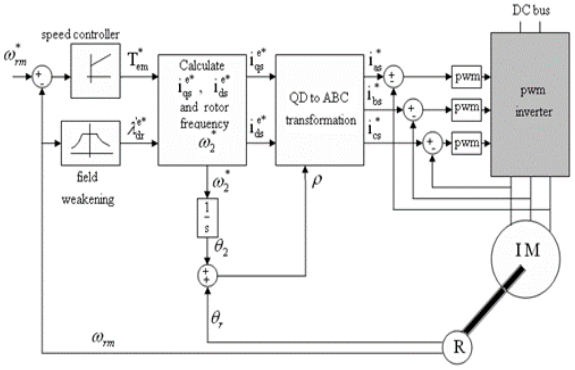


*Fig. 9 Indirect field-oriented control of a current regulated induction motor drive.*

Figure 9 shows an indirect field-oriented control scheme for a current controlled PWM induction motor drive. The field orientation, ρ, is the sum of the rotor angle from the position sensor $\theta_r$, and the angle $\theta_2$,

from integrating the slip speed. If orthogonal outputs of the form $\cos\theta_r$ and $\sin\theta_r$ are available from the shaft encoder, the values of $\cos\rho$ and $\sin\rho$ can be generated from the following trigonometric identities:

$$\cos\rho = \cos(\theta_r + \theta_2) = \cos\theta_r \cos\theta_2 - \sin\theta_r \sin\theta_2 \quad (18)$$

$$\sin\rho = \sin(\theta_r + \theta_2) = \sin\theta_r \cos\theta_2 - \cos\theta_r \sin\theta_2 \quad (19)$$

In simulation, the value of $\cos\theta_2$ and $\sin\theta_2$ may be generated from a variable-frequency oscillator.

For the proposed inverter switching requirements can be stated as follows. Given a desired set of three-phase voltages and a set of three-phase currents for the output inverter:

$$v_{01} = V_0 \sin\omega t \quad (20)$$

$$v_{02} = V_0 \sin\left(\omega t - \frac{2\pi}{3}\right) \quad (21)$$

$$v_{03} = V_0 \sin\left(\omega t + \frac{2\pi}{3}\right) \quad (22)$$

$$I_{01} = I_0 \sin(\omega t - \theta) \quad (23)$$

$$I_{02} = I_0 \sin\left(\omega t - \theta - \frac{2\pi}{3}\right) \quad (24)$$

$$I_{03} = I_0 \sin(\omega t - \theta + \frac{2\pi}{3}) \quad (25)$$

where V, and I, are the magnitudes of the output voltages and currents, respectively.

$$v_{01n} = v_{01} - v_{03} = \sqrt{3}V_0 \sin(\omega t - \frac{\pi}{6}) \quad (26)$$

$$v_{02n} = v_{02} - v_{03} = \sqrt{3}\,V_0 \sin(\omega t - \frac{\pi}{2}) \quad (27)$$

where n is the DC bus centre point assumed to be ground.

## 4. FUZZY LOGIC CONTROL

In Fuzzy logic control (FLC), basic control action is determined by a set of linguistic rules. These rules are determined by the system. Since, the numerical variables are converted into linguistic variables, mathematical modelling of the system is not required in FLC [3]. The FLC comprises of three parts: fuzzification, interference engine and defuzzification. The FLC is characterized as,

i. Seven fuzzy sets for each input and output.
ii. Triangular membership functions for simplicity.
iii. Fuzzification using continuous universe of discourse.
iv. Implication using Mamdani's min operator.
v. Defuzzification using the "height" method.

To convert the numerical variables into linguistic variables, the fuzzy levels chosen are NB (negative small), NM (negative medium), NS (negative small), ZE (zero), PS (positive small), PM (positive medium) and PB (positive big). The value of input error E(K) shown in figure 10and change in error CE(K) shown in figure 11 are normalized by an input scaling factor. In this system the input scaling factor has been designed such that input values are between -1 and +1. The triangular shape of the membership function of this arrangement presumes that for any input there is only one dominant fuzzy subset.

$$C(K) = E(K) - E(K-1) \quad (28)$$

In the present work, for fuzzification, non-uniform fuzzifier has been used. If the exact values of error and change in error are small, they are divided conversely and if the values are large, they are divided coarsely.

Table.1. Fuzzy rules

| CE \ E | NB | NM | NS | ZE | PS | PM | PB |
|---|---|---|---|---|---|---|---|
| NB | NB | NB | NB | NB | NM | NS | ZE |
| NM | NB | NB | NB | NM | NS | ZE | PS |
| NS | NB | NB | NM | NS | ZE | PS | PM |
| ZE | NB | NM | NS | ZE | PS | PM | PB |
| PS | NM | NS | ZE | PS | PM | PB | PB |
| PM | NS | ZE | PS | PM | PB | PB | PB |
| PB | ZE | PS | PM | PB | PB | PB | PB |

$$U = -[\alpha E + (1-\alpha) * C] \quad (29)$$

Where α is self-adjustable factor which can regulate the whole operation. E is the error of the system; C is the change in error and U is the control variable shown in figure 12. A large value of error E indicates that given system is not in the balanced state. If the system is unbalanced, the controller should enlarge its control variables to balance the system as early as possible. One the other hand, small value of the error E indicates that the system is near to balanced state. Overshoot plays an important role in the system stability. Less over-shoot is required for system stability and in restraining oscillations. C plays an important role, while the role of E is diminished. The optimization is done by α.

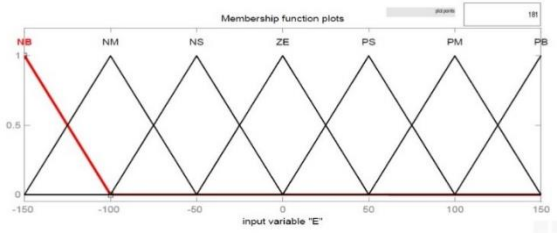


Fig. 10 Triangular wave form for fuzzy input variable E

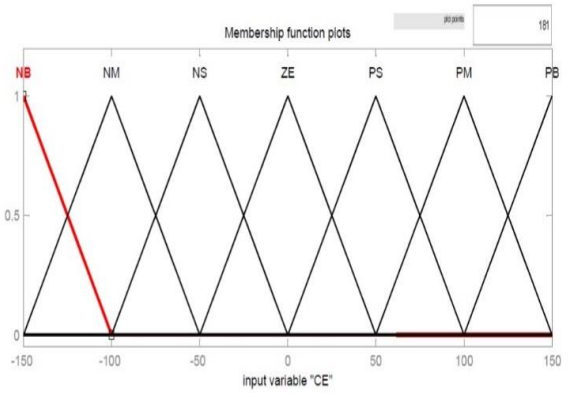


Fig. 11 Triangular waveform for fuzzy input variable CE

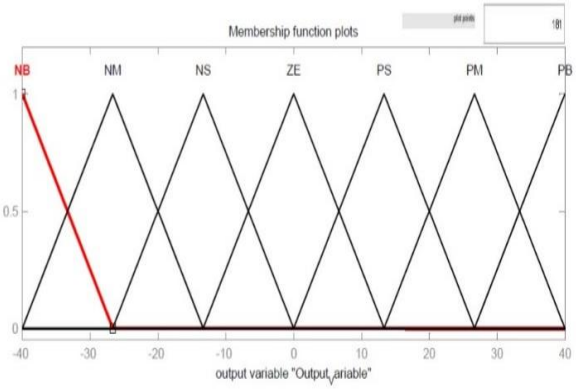


Fig. 12 Triangular waveform for Fuzzy output variable

## 5. SIMULATION RESULTS

A three-phase 5hp Induction motor with the specifications given in the appendix section has been used in this simulation. The MATLAB model of the single-phase to three-phase converter is simulated and the results is shown in the below figures(13-21) for the given three-phase induction motor. The output line voltages, three-phase output currents, speed ($\omega_m$), Electromagnetic torque (Nm) and THD for the input current.

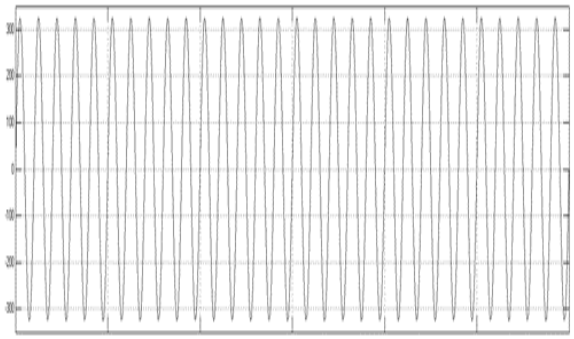

Fig. 13 Input source voltage

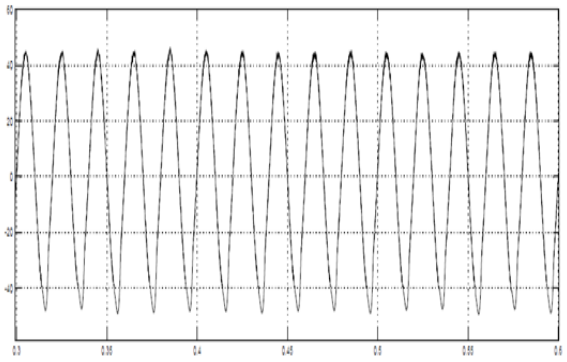

Fig. 14 Source current

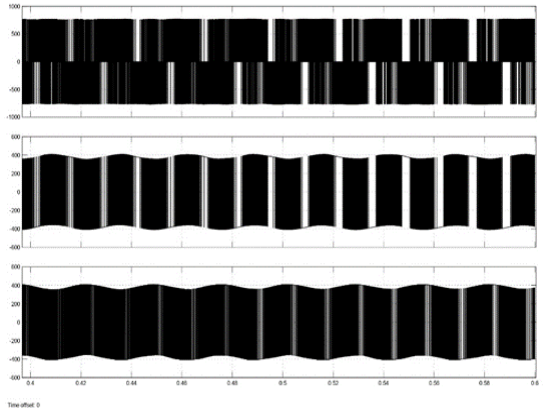

Fig. 15 Three-phase Inverter output voltages

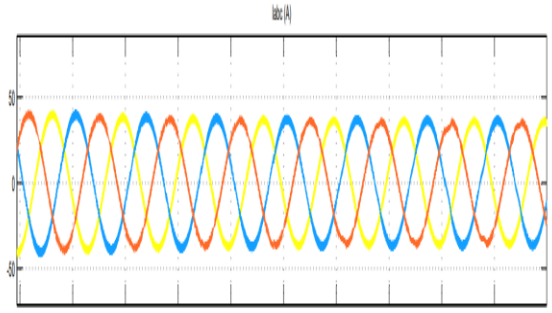

Fig. 16 Induction motor input currents

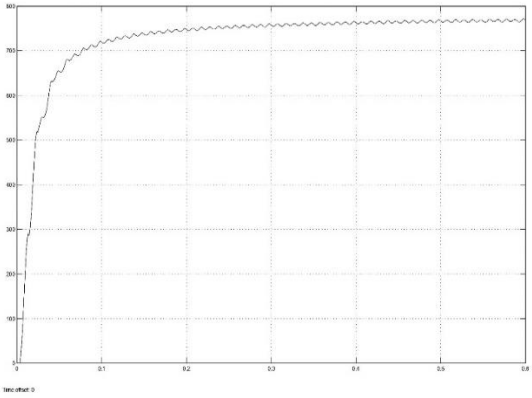

Fig. 17 DC-Link voltage with PI controller

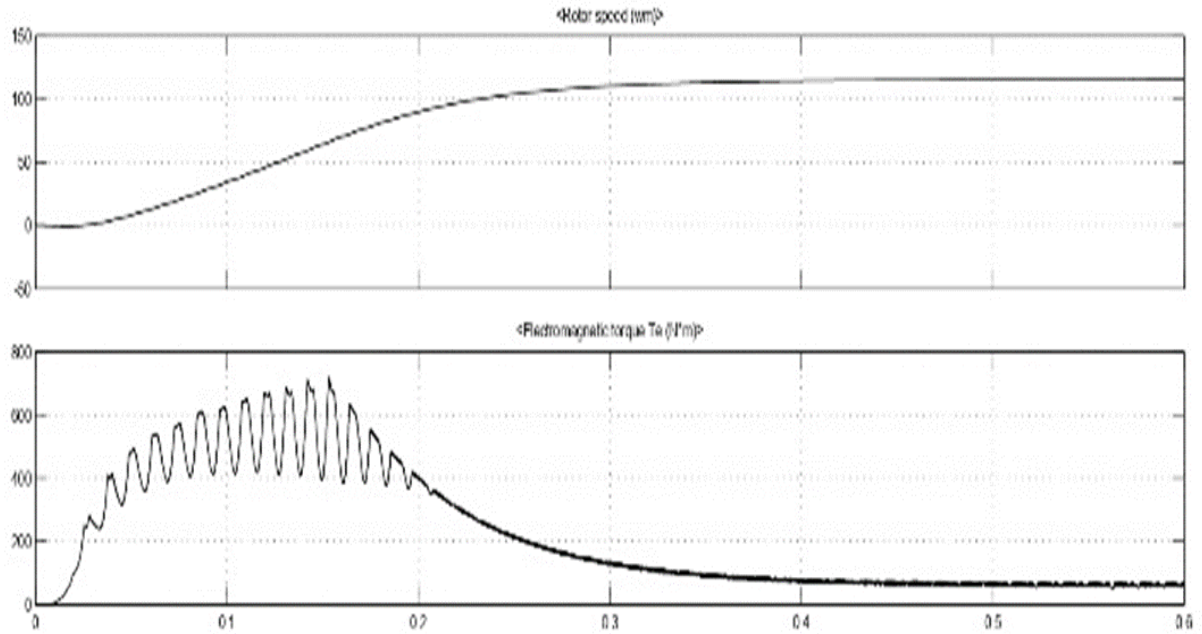


Fig. 18 Motor speed and Electromagnetic torque

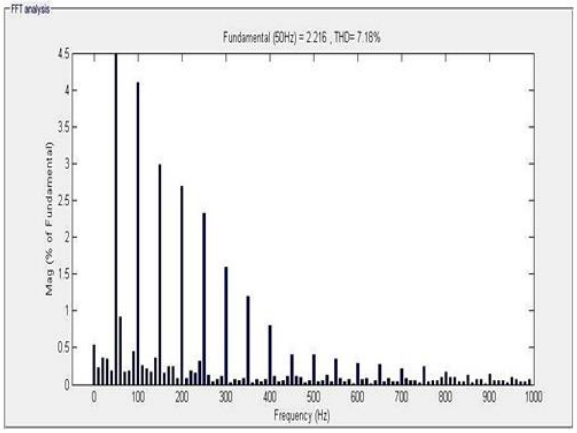


Fig. 19 FFT input current of the front-end rectifier using pi controller

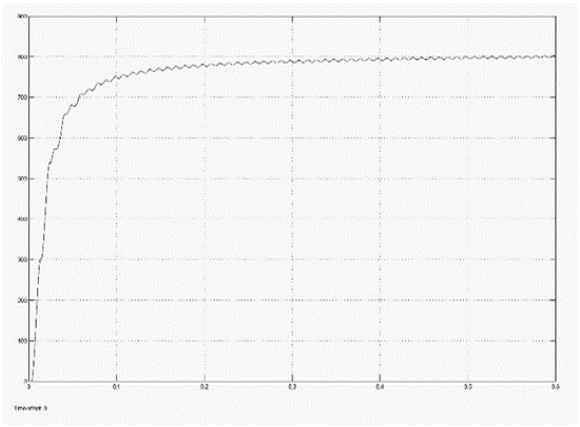

Fig. 20 DC-Link voltage with FLC controller

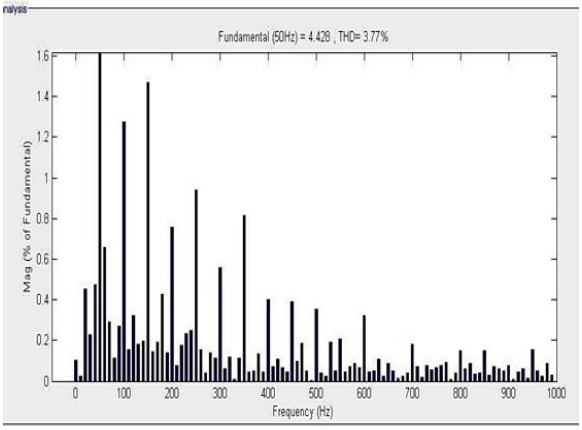


Fig. 21 FFT input current of front-end rectifier using fuzzy logic control strategy.

The load torque has been set at 50 N-m. The simulation results of the induction motor drive fed by four switch inverter with voltage control. The angular speed of the motor is 120 rad/sec. The output of four switch inverter is a three-phase balanced voltage. The Fig. 16 shows induction motor input current 40 Amperes. The DC-Link voltage 800 Volts is maintained constant.

The DC-link voltage response with PI controller and Fuzzy controller has been shown in figure 17 & 20 respectively. Comparatively the Fuzzy logic controller shows the good response. The parameters like rise

time, settling time and steady state error has been calculated and shown in below tabular column.

Table. 2 Comparison of Parameters between PI controller and Fuzzy controller

| Parameter | PI controller | Fuzzy controller |
|---|---|---|
| Rise time (Sec) | 0.0983 | 0.06995 |
| Settling time (Sec) | 0.5 | 0.46 |
| Steady state error (%) | 3.75 | 1.25 |

The performance of the converter model is compared by incorporating PI controller and Fuzzy logic controller. From the figures 14 - 20 the values are tabulated in the table 3 its observed that the parameters like torque ripple, converter output current and DC link voltage has shown good response with fuzzy logic controller compared to PI controller.

Table. 3 Comparison of system parameters with PI controller and Fuzzy controller

| Parameter | PI controller | Fuzzy logic controller |
|---|---|---|
| Speed (RPM) | 1100 | 1100 |
| Converter output current RMS (A) | 27.5 | 28.2 |
| Torque (Nm) | 50 | 50 |
| Torque ripple (%) | 24 | 22 |
| DC-link voltage (Volts) | 770 | 790 |

The Total harmonic distortion for the input source current of the converter controlled by PI controller and Fuzzy controller shown in figures 19 & 21 respectively is given in below tabular column.

Table. 4 THD Comparison of input source current

| Parameter | PI controller | Fuzzy controller |
|---|---|---|
| THD (%) | 7.18 | 3.77 |

The FFT analysis of the proposed converter operated with PI controller is 7.18 % and when operated by Fuzzy logic controller is 3.77 %.

## 6. CONCLUSION

This work presents a single-phase to three-phase converter for controlling the speed of an induction motor. This converter controls the output voltage with fixed frequency. The minimum components are used in this scheme, which effectively decreases cost. This converter also provides voltage boost capability and active current shaping. This converter reduces line (utility) harmonics and regulates DC-link voltage in a high value. The control strategies for front end rectifier using PI control technique and Fuzzy logic control strategy is compared. Comparatively front-end rectifier operated with fuzzy logic control has shown better results in FFT analysis.

Appendix

Table. 5 Induction motor parameters referred to stator.

| | |
|---|---|
| $R_s$ (Ω) | 0.087 |
| $R_r$ (Ω) | 0.228 |
| $X_{ls}$(Ω) | 0.251 |
| $X_{lr}$(Ω) | 0.251 |
| $X_m$(Ω) | 10.916 |
| $V_{(rms)}$ (volts) | 400 |
| Base frequency(Hz) | 50 |
| Number of pole pairs | 2 |
| Inertia(Kg.m$^2$) | 0.831 |
| Friction(Nm.s) | 0.1 |
| Rated power(hp) | 5 |

## REFERENCES

[1] Vaibhav S. Chandekar; M.A. Chaudhari; V. Kalyan Chakravarthi, “A Low cost three phase induction motor drive operated on single phase input source, “in International Conference on Smart Electric Drives and Power System., June 2018, DOI: 10.1109/ICSEDPS.2018.8536009.

[2] E. Cipriano dos Santos. C. B. Jacobina, E. R. Cabral da Silva, N. Rocha,” Single-phase to three-phase power converters: state of the art”, IEEE transaction 0885-8993, 2011.

[3] Chirag Patel and R. Mahanty,” Fuzzy Logic Controlled Unified Power Quality Conditioner for Power Quality Improvement,” 16th NATIONAL POWER SYSTEMS CONFERENCE., December 2010, pp. 681-686.

[4] V. Kinnares and C. Charumit, ‘‘Modulating functions of space vector PWM for three-leg VSI-fed unbalanced two-phase induction motors’’,

IEEE Trans. Power Electron. vol. 24, no. 4, pp. 1135-1139, Apr. 2009.

[5] Dong-Choon Lee, Young-Sin Kim, 'Control of single-phase-to-three-phase AC/DC/AC PWM converters for induction motor drives', IEEE Trans. Ind. Electron., 2007, 54, (2), pp. 797–804.

[6] P.Marino, M.D'Incecco and N.Visciano," A comparison of Direct Torque Control Methodologies for Induction Motor", IEEE transaction 2001

[7] A.M. Trzynadlowski, "Control of Induction Motors", Academic Press, 2001.

[8] T. Bon, L.F. Backer "Serving large electric motors with single-phase power", North Dakota power use council, fall 1996.

[9] B. R. Lin and T. S. Huang, "Single Phase Rectifier with High Power Factor in Discontinuous Conduction Mode", IEEE international Symposium on Industrial Electronics, pp. 421 - 426, 1995.

[10] P.Enjeti, and A. Rahman," a new single phase to three phase converter with active input current shaping for low-cost ac motor drives," IEEE Trans. Ind.Appl., vol.29, no.4, pp.806-813, Jul.1993.

[11] P.Enjeti, A. Rahman, and R. jakkli," Economic single phase to three phase converter topologies for fixed and variable frequency output," IEEE Trans. Power Electron. Vol. 8 no. 3 pp.88-94 Jul.1993

[12] P.Enjeti, A. Rahman, and R. jakkli," Economic single phase to three phase converter topologies for fixed frequency output," in Proc.6th Annual. Power electron. Conf.Expo. Mar. 1991 pp.88-94

[13] Heinz W. Van Der Broeck, Jacobus D. Van Wyk," A Comparative Investigation of a Three-Phase Induction Machine Drive with a Component Minimized Voltage-Fed Inverter under Different Control Options" IEEE Trans. Industry Applications, vol. IA-20, no. 2, pp. 309-320, Mar./Apr. 1984.